

# Field Study of Load Path in Rail and Concrete Crosstie System

Justin S. GRASSE, Sihang WEI, J Riley EDWARDS, Daniel KUCHMA, David A. LANGE\*  
*University of Illinois at Urbana-Champaign, Urbana, Illinois, USA*

\*dlange@illinois.edu

**ABSTRACT:** The design and performance of concrete ties and elastic fastening systems must be improved to meet demands placed on North America's railway infrastructure through ever-increasing freight tonnages and development of its high speed rail program. In July 2012, a field experimentation program was performed at the Transportation Technology Center (TTC) in Pueblo, CO by researchers from the University of Illinois at Urbana-Champaign (UIUC). This paper focuses on the transfer of vertical and lateral loads through the system, demonstrating the demands of the fastening components (e.g. insulators, fastening clips) and concrete crossties. Measurements of loads, strains and displacements were used to quantify the physical response of the system under various parameters (track curvature, train speed, and car weight). The experimental data provide validation for a comprehensive finite element model developed by UIUC. Improvements to instrumentation strategies and areas of uncertainty will also be discussed. These experimental results will be used to guide future research in further quantifying the field loading demands, ultimately leading to a mechanistic design approach for the concrete crosstie and components within the fastening system.

*Keywords: Railway infrastructure, concrete crosstie, fastening system, vertical wheel load, lateral wheel load*

## 1 INTRODUCTION

Concrete crossties provide excellent durability and capacity, which allow them to outlast standard timber crossties in tracks with high degrees of curvature and extreme weather exposure [1]. Concrete crossties also offer improved track geometry retention for high speed rail and heavy freight lines [2].

Concrete crossties are experiencing a wide variety of failure mechanisms with the continual increase in annual gross tonnages. In North America, the most common failure mode is rail seat deterioration (RSD) — the wearing out of the concrete within the rail seat [3]. North American Railroads ranked RSD as the most critical problem facing concrete crosstie track [4]. Individual components of the fastening system can fail from fatigue and abrasion mechanisms. Wear or failure of the fastening clips, shoulders, and insulators allow additional movement in the system and lead to further deterioration.

Component behavior and system demands must be investigated in order to better understand the behavior of the crosstie-fastener system. This includes an understanding of load transfer among each component. There is a need for the magnitude of these input loads with respect to the train speed, car weight, track curvature, grade, and various fastening systems [5]. Obtaining these measurements syn-

chronously from field tests will provide insight into the more complex interactions and lead to a more purposeful, mechanistic design approach of the system.

The University of Illinois at Urbana-Champaign (UIUC) formulated a comprehensive field experimental program to pursue a mechanistic design approach. The program conducted in July 2012 used strain gauges (surface and embedment), linear potentiometers, and matrix based tactile surface sensors (MBTSS). The full-scale field experiment provided vertical and lateral loads, rail movements, crosstie displacements, and stresses within the clip and insulator. Loads were applied by the Transportation Technology Center (TTC) using a passenger consist, freight consist, and a specialized Track Loading Vehicle (TLV). The well-characterized tests allowed for a comprehensive analysis of the vertical and lateral load paths.

## 2 OBJECTIVES

The primary objective was to characterize the overall behavior and quantify the demands placed on individual components in the crosstie and fastening system under varying conditions. The analysis aimed to provide new understanding of the vertical and lateral load paths by mapping the magnitude of

stresses at different interfaces (e.g. rail seat forces) and determining influencing factors. The load path mapping ultimately aided in the mechanistic design of the system: a design strategy dependent on both analytical and scientific principles. [6] Although it has not been a focus of the railroad industry in recent years, mechanistic design has been a common approach in many disciplines, including the design of highway pavements. [7] Additionally, this experimentation provided validation for a computational model developed by the UIUC. This 3-D finite element model will be composed of multiple cross-ties and a detailed fastening system in order to perform quick parametric analyses (e.g. the effects of fastener types on system performance).

### 3 FIELD INSTRUMENTATION

In July 2012, two sections of track were investigated at TTC in Pueblo, CO. One test section was on tangent track and one on curved track with a curvature of approximately 5°. In both sections, 15 new concrete cross-ties were installed with new ballast, exposed to fewer than 0.1 million gross tons [MGT]. The loading environment consisted of a passenger consist, freight consist, and TLV for static loading and calibration.

#### 3.1 Vertical Wheel Loads

Vertical wheel loads were determined using an arrangement of strain gages in the crib of the rail (Figure 1). Weldable strain gages were assembled in a Wheatstone bridge and calibrated with a TLV. Gages were placed in a chevron pattern at the neutral axis of the rail section as shown, oriented at 45°. The centers of the two groups of gages were measured at 5" from each side of the center of the crib. This has served as a commonly used methodology for deter-

mining accurate measurements of vertical wheel loads since its development in the 1970's. [8]

The vertical load,  $P_z$ , can be determined by the difference of shears in each plane:

$$P_z = V_{ZL} - V_{ZR} \quad (1)$$

The shear forces at each face ( $V_{ZL}$  and  $V_{ZR}$ ) can be calculated as follows:

$$V_{ZL} = \frac{EI}{(1 + \nu)Q} \epsilon_1 \quad (2)$$

$$V_{ZR} = \frac{EI}{(1 + \nu)Q} \epsilon_2 \quad (3)$$

where  $E$  is the steel modulus of elasticity,  $I$  is the moment of inertia of the rail cross-section,  $\nu$  is the Poisson's ratio,  $Q$  is static moment of area, and the principal strains ( $\epsilon_1$  and  $\epsilon_2$ ) are comprised of the strains shown in red in Figure 1.

$$\epsilon_1 = \epsilon_a - \epsilon_b + \epsilon_{a'} - \epsilon_{b'} \quad (4)$$

$$\epsilon_2 = \epsilon_c - \epsilon_d + \epsilon_{c'} - \epsilon_{d'} \quad (5)$$

Thus, the load  $P_z$  could be rewritten as:

$$P_z = \frac{EI}{(1 + \nu)Q} (\epsilon_1 - \epsilon_2) \quad (6)$$

Eliminating all the constants, the load  $P_z$  is proportional to the recorded strain from the bridge, allowing for characterization of load with proper calibration:

$$P_z \propto (\epsilon_1 - \epsilon_2) \quad (7)$$

The strains  $\epsilon_1$  and  $\epsilon_2$  can be obtained by using a Wheatstone bridge. The strain difference ( $\epsilon_1 - \epsilon_2$ )

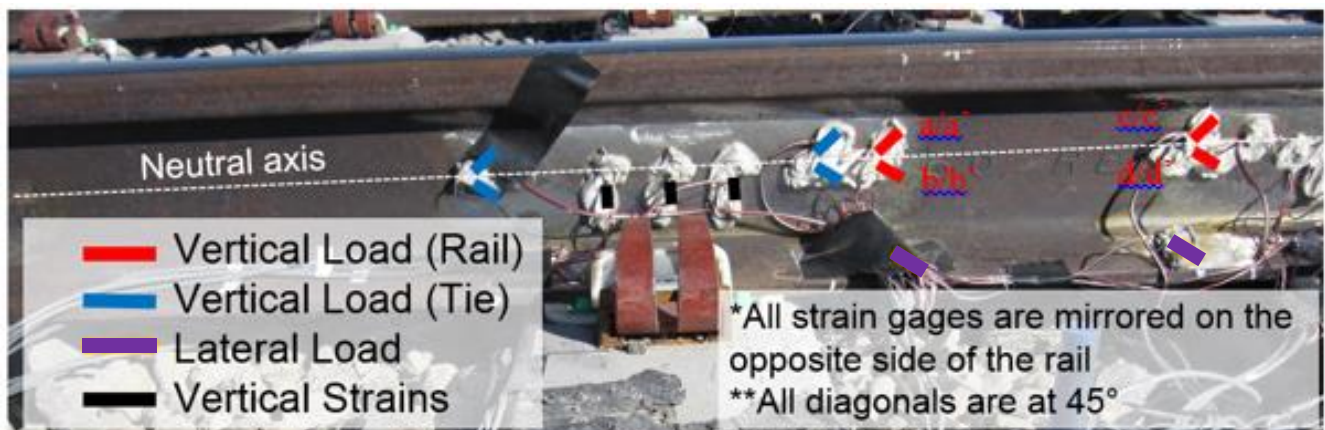


Figure 1. Strain gage configurations for load circuits.

can be measured directly by including each strain gage into the Wheatstone bridge.

### 3.2 Rail Seat Loads

Vertical rail seat loads were determined using the same arrangement of strain gages on the rail web as the vertical circuits, but located directly above the rail seat (Figure 1). Weldable strain gages were assembled in a Wheatstone bridge and the calibration from the crib was used to capture the shear difference across this circuit. The rail seat forces were determined by taking the difference of this measurement and an adjacent vertical wheel load measured in the crib.

### 3.3 Lateral Wheel Loads

Lateral wheel loads were determined using an arrangement of strain gages in the crib of the rail (Figure 1). Instead of measuring shear in the vertical directions, these shear strains were rotated about the rail section and positioned on the rail base in order to measure shear in the direction of the lateral loads.

### 3.4 Lateral Rail Displacements

Lateral rail displacements were measured at the rail base and the neutral axis of the rail relative to the crosstie using linear potentiometers. These measurements captured the lateral movement and stiffness of the system. The potentiometers used to measure lateral displacements were screwed onto a small aluminum plate epoxied to the crosstie (Figure 2).

### 3.5 Global Vertical Crosstie Displacements

Global vertical displacements of the crosstie were

measured with linear potentiometers affixed to 6' rods driven through the track substructure into the subgrade. These measurements were taken at the two ends of a crosstie (seen in the forefront on the right of Figure 2). These measurements captured the local stiffness of the substructure.

### 3.6 Vertical Rail Strains

Vertical rail strains were measured near the base of the web. A vertical strain gage was centered on each side of the rail, 2" above the rail base. These strains demonstrated the stress distribution of the rail along a stretch of seven crossties.

## 4 FINDINGS

The study provided new insight into the load path in the fastening system. Discussion of the vertical load path and lateral load path are discussed below.

### 4.1 Vertical Load Path

The highest load demands were vertical loads, especially with heavy freight traffic and impact loads which result from wheel profile imperfections and dynamic truck behavior. There is significant need to understand how this load is being transmitted through the system and shared between adjacent crossties and the many factors that contribute to demands (e.g. track modulus, track curvature).

#### 4.1.1 Vertical Wheel Loads

Vertical wheel loads are the vertical components of the wheel force acting on the head of the rail. The static load of a wheel due to car weight is called the nominal wheel load, defined as "the vertical load on the rail from a wheel when measured on level tangent track". [9] The vertical load of the wheel on

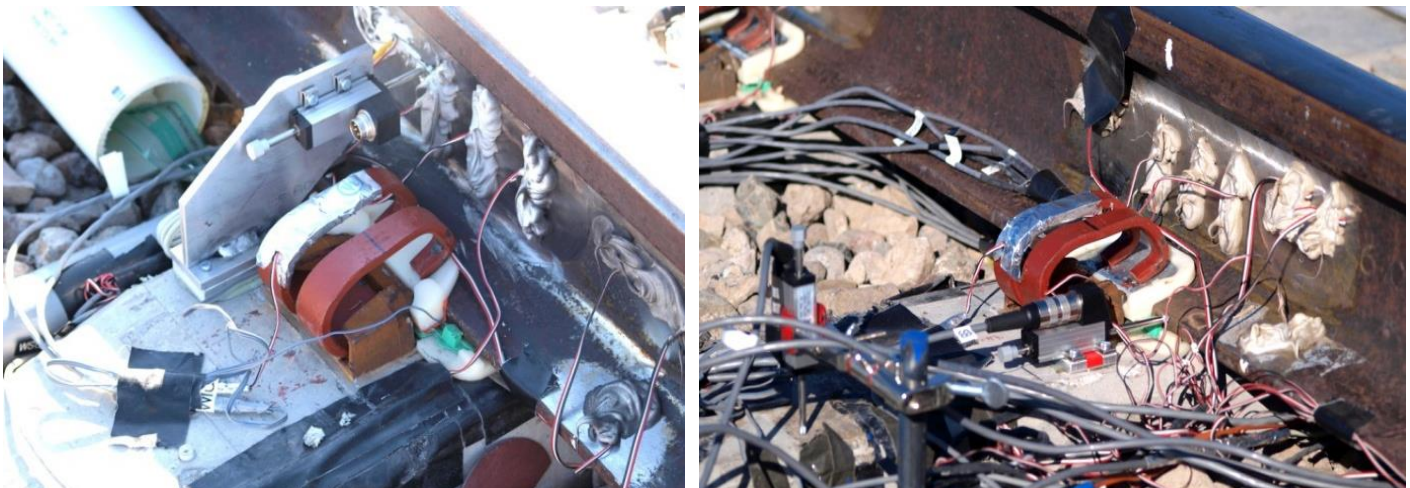


Figure 2. Position of linear potentiometer on the rail web (left) and rail base (right).

the rail often deviates depending on train speed and track curvature. In extreme cases vertical wheel loads, called impact loads, far exceed nominal wheel loads primarily due to wheel flats which allows for little damping of the track structure. [10]

Vertical loads at TTC were measured from a freight consist which consisted of cars weighing 263, 286, and 315 kips with nominal wheel loads of 33, 36, and 39 kips respectively. Median vertical loads from this freight consist on tangent track were approximately 35 kips (Figure 3). With the exception of one load of 60 kips, these magnitudes do not exceed 25% of the nominal wheel load. There is also negligible correlation between the average vertical wheel loads on tangent track and train speeds. However, there is an increase in maximum loads (excluding one 60 kip impact load at 30 mph) from increased vehicle dynamics.

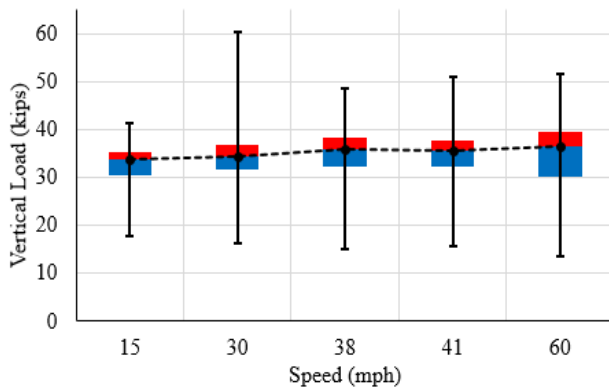


Figure 3. Vertical wheel loads imparted by a freight consist on tangent track.

The vertical wheel loads measured on curved track are higher and dependent on curve radius. Additional loading demands on the high rail arise from overbalanced speeds due to centrifugal forces acting on the body of the vehicle. Conversely, underbalanced speeds increase the loading demand on the low rail as the superelevation causes the center of gravity to shift nearer to the low rail. Both these extremes are cited as potential contributors to the current failure modes of concrete cross-ties, specifically rail seat abrasion. (13)

The measured vertical loads imparted by the freight consist on a curved track (balancing speed of 33mph) showed the dependency of forces on train speed (Figure 4). The low rail experienced a modest reduction, and the high rail experienced a slight rise in vertical wheel load with increasing speed. At an overbalanced speed of 45 mph, there was a significant increase in the median vertical wheel loads on the high rail (approximately 40% higher than the average nominal wheel loads), which far exceeds the expected loading demands on tangent track. This suggests that there may be a benefit of treating tan-

gent and curved sections of track separately in design. This could include using specialized components or practices to compensate for the increase loading demands (e.g. more robust fasteners or tighter tie spacing). Also at an overbalance speed of 45 mph, there was a significant reduction in vertical loads on the low rail (approximately 20% lower than the average nominal wheel load). This poses a different obstacle to design, in that there is an increased lateral to vertical load (L/V) ratio which demands more lateral and rotational restraint, presuming the lateral force remains relatively consistent.

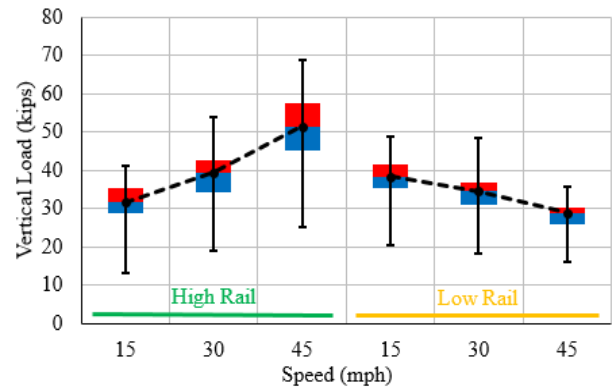


Figure 4. Vertical wheel loads imparted by a freight consist on curved track.

Vertical loads were measured from a passenger consist, which consisted of cars weighing 87 kips with nominal wheel loads of 11 kips. Median vertical loads from this passenger consist on tangent track did not deviate much from the nominal wheel loads (11-12 kips, Figure 5). However, there were considerably higher impacts measured as high as 2.5 times the nominal wheel load. Approximately 3% of the vertical loads measured exceeded 1.5 times the nominal wheel load, and 0.5% of the loads exceeded 2.5 times the nominal wheel load from eighteen train passes on tangent track (2-102 mph).

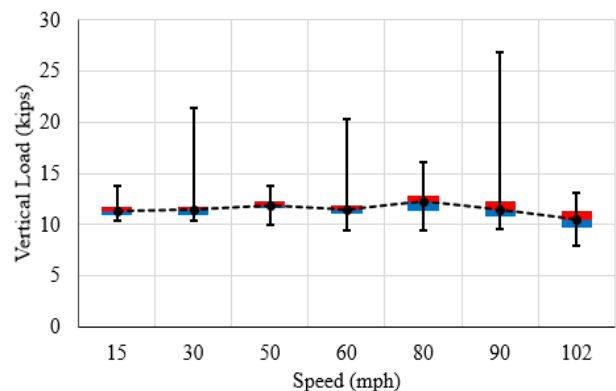


Figure 5. Vertical wheel loads imparted by a passenger consist on tangent track.

#### 4.1.2 Vertical Crosstie Deflections

Track deflections are recognized as being a primary indicator of predicting track strength and quality. (14) In the railroad industry, a commonly used measure of substructure stiffness is the modulus of track elasticity, or track modulus. Track modulus is defined as “the load per unit length of rail required to depress that rail by one unit”. (15)

Although track modulus represents an all-encompassing value of substructure stiffness, there are more local phenomena that cause variability in the mechanics, such as inconsistent support conditions from gaps within the ballast structure. Adjacent ties experienced between 50-85% of the center crosstie displacement with 40 kips of static vertical load applied on a single crosstie.

Different distributions were seen on the low and high rail of the curved track (Figure 6). The low rail showed the highest displacement of 0.14”, which far exceeded the optimum displacement (0.05”) for quality concrete track as well as the average deflection of the track used in calculating track modulus. (14) These high displacements are evidence of low substructure (ballast, subballast, and subgrade) stiffness and could be a result of inconsistency in a non-uniformly tamped section with negligible tonnage. A range of nine ties were being engaged (showing measurable stresses) at the ballast interface on the low rail. Assuming a direct relationship between displacement and load distribution (i.e. a consistent value of substructure stiffness), the center tie of this section sustained approximately 20% of the load, while the center three crossties sustained a total of 50% of the load at the ballast interface.

The high rail showed indications of stronger substructure stiffness, generating displacements 40% less than the displacements at the low rail. Approximately five to seven crossties were being engaged

at the ballast interface. The center tie of this section sustained approximately 30% of the load and the center three crossties sustained a total of 70% of the load, assuming a consistent track modulus.

#### 4.1.3 Rail Seat Loads

Rail seat loads are the forces distributed to the concrete rail seats below the rail. In practice, this rail seat load as a percentage of wheel load is commonly approximated as 50% for 24” tie spacing. (15) Recent tests concluded that this transfer load was approximately 57% for a similar spacing. (16) AREMA also estimates the transfer load for 24” tie spacing to be just above 50%. (17)

The rail seat loads as a percentage of the wheel load showed significant variability over adjacent ties, which correlates with track stiffness (Figure 7). The average rail seat load transfer measured from the freight consist over tangent track varied from 15 to 50%. The three adjacent rail seats had similar load transfers (about 40-50%) and the ends of the crossties at those locations showed deflections of approximately 0.06”. The rail seat on the opposite end of the center crosstie had a considerably lower transfer of load (about 13%) and a vertical deflection of 0.12”, evidence of low substructure stiffness. There is increased flexure in the rail from a more compliant substructure and a potential gap between the tie and ballast. This allows for more of the vertical load to be transferred to adjacent rail seats as well as the strain energy associated with bending of the rail.

Rail seat loads were plotted against vertical crosstie displacements from static tests (Figure 8) to illustrate their dependency on support conditions. The high rail showed characteristics of high track modulus, while the low rail showed characteristics of low track modulus. The rail seat on the high rail showed

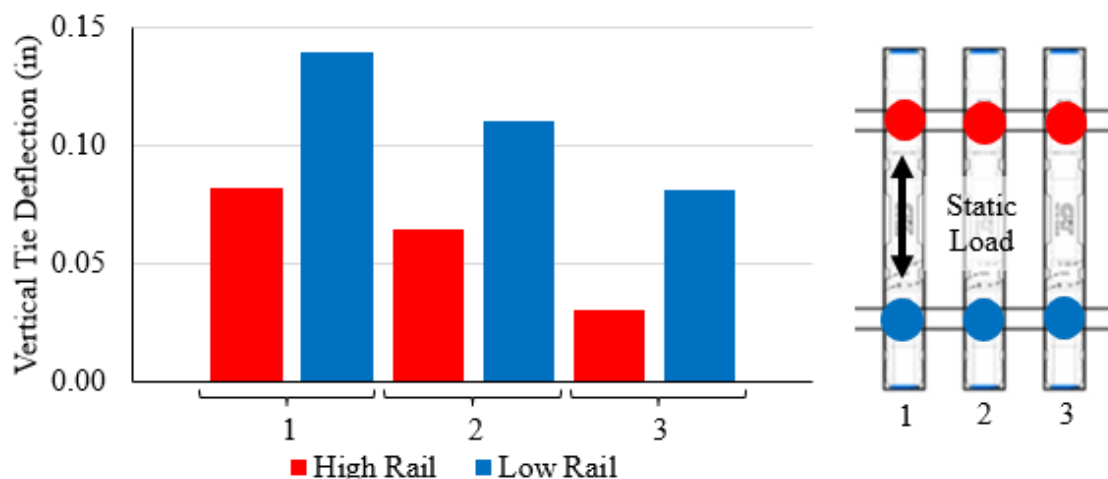


Figure 6. Vertical deflections of adjacent crossties under static loading.

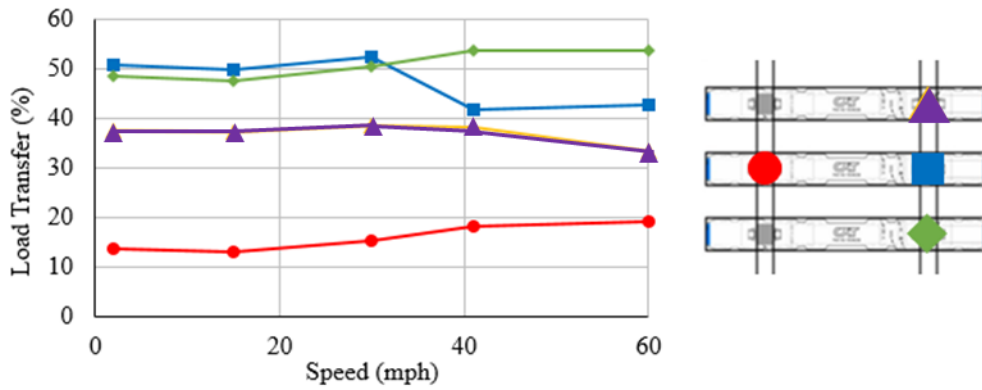


Figure 7. Percentage of load being transferred into the crosstie

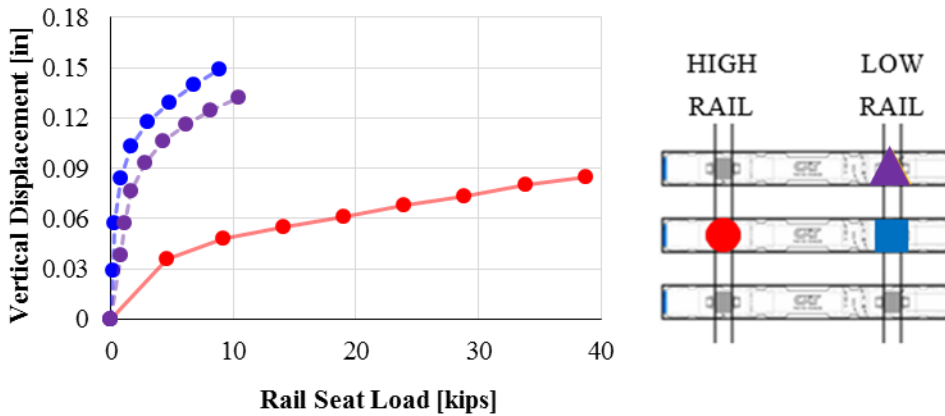


Figure 8: Crosstie displacements and rail seat loads from static vertical loading

low displacements, resulting in higher rail seat loads. Conversely, the rail seats on the low rail with high displacements showed low rail seat loads. The rail is allowed to displace significantly before the rail seat is fully engaged with weak support. This initial and dramatic increase in displacement represents a gap in which the crosstie is not fully engaged until it displaces enough to eliminate slack in the system.

#### 4.1.4 Vertical Load Distribution

Vertical load distribution was explored using the vertical crosstie displacements and rail seat loads. The center crosstie on the low rail of curved track made up 20% of the stresses at the crosstie-ballast interface and 25% of the forces at the rail seat. This magnitude of load percentages suggested that about seven to nine crossties are being engaged and that there is damping within the system.

Vertical load distribution was investigated at the rail level using the vertical web strains. The relative distribution of rail stresses showed that the load was less distributed in the high rail (Figure 9) than in the low rail (Figure 10) in response to a static load of 40 kips vertical and 20 kips lateral.

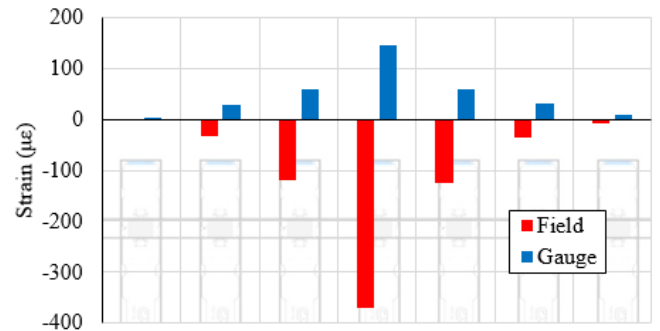


Figure 9. Strains in high rail from 40kips vertical and 20kips lateral load.

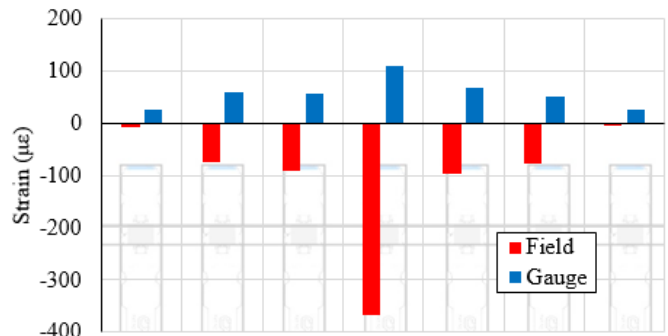


Figure 10. Strains in low rail from 40kips vertical and 20kips lateral load.

There was approximately 66% of load being transferred over the center tie on the low rail from the 40 kip vertical load and 63% from the 40 kip load with the additional 20 kip lateral load. These percentages demonstrate the concentration of stresses in the web before being further distributed through the flange and are much greater than the 20% and 25% transfer loads determined by the vertical crosstie displacements and rail seat load methodology, respectively.

#### 4.2 Lateral Load Path

Lateral loads are the most demanding on the fastening system. In particular, lateral loads apply large bending moments to the rail, which requires rotational restraint from the fastening system. (5) In recent years, the lateral load path through the cross-tie-fastener system has gained considerable interest in order to mitigate problems such as rail seat abrasion, shoulder wear, insulator post failure, etc. These lateral demands are influenced mainly by curve radius, train speed, wheel-rail interface, and suspension characteristics of the trucks. (18)

##### 4.2.1 Lateral Wheel Loads

On tangent track, most axles imposed a modest outward lateral load to the rail. From the freight consist these loads were approximately 2.5 kips. In addition, there were negative (inward towards the gauge) or negligible loads observed, representing about 20% of the total lateral loads measured from twelve train passes from train speeds of 2 to 45 mph. Over 75% of the outward lateral loads from freight were below 3.5 kips. One in about forty axles imparted approximately a 6 kip lateral load. However, on tangent track, there was negligible correlation between lateral loads and train speed. This suggests that train speed should not be a heavily weighted in the design of tangent track.

Median lateral loads on curved track from the freight consist were significantly greater (2-5 times as large on average, Figure 11 and Figure 12). Additionally, lateral loads on curved track were heavily dependent on train speed. Lateral loads nearly doubled on the high rail as the balancing speed (about 33mph) was exceeded. On the low rail, there was a slight reduction in median lateral loads, while maximum loads remained unchanged. The differences in magnitude of lateral demands on each track type suggest that there should be significantly higher lateral loading demands on curved than tangent track in design.

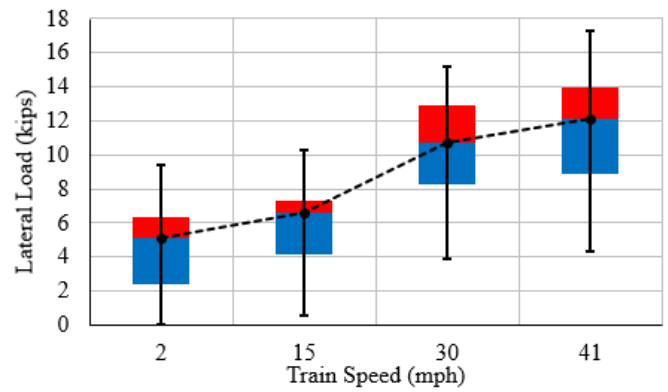


Figure 11. Lateral wheel loads imparted by a freight consist on the high rail.

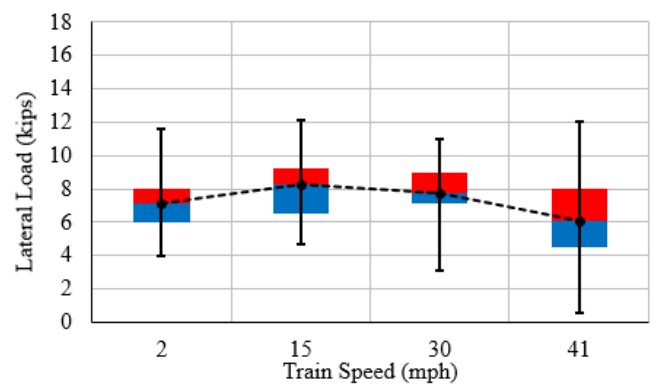


Figure 12. Lateral wheel loads from a freight consist on the low rail.

It is worth developing a way to develop design lateral loads (e.g. from the design vertical loads) in design of fastening systems. In order to observe the dependency of lateral loads on vertical loads, each load was plotted for each axle of a freight consist travelling at various speeds on tangent and curved track.

On tangent track, there was no strong correlation between concurrently acting vertical and lateral wheel loads. On curved track, however, there was an evident relationship. On the high rail, there was a positive correlation between lateral and vertical wheel loads. The low rail showed a slight negative correlation between lateral and vertical loads.

The trendlines showing correlation between lateral and vertical loads on the high and low rail are shown in Figure 13. These lines represent the range of concurrent lateral and vertical loads from similarly weighted railcars. Around the balancing speed (about 30mph), the vertical loads on the high and low with no lateral load converged to 35kips (about the 36kip nominal wheel load). On the low rail, as the lateral loads increased there was less concurrently acting vertical load. This translates to a higher L/V ratio, which imparts higher bending forces with

less normal forces to “pin” the rail. This places increased lateral and rotational demands on the fastening system.

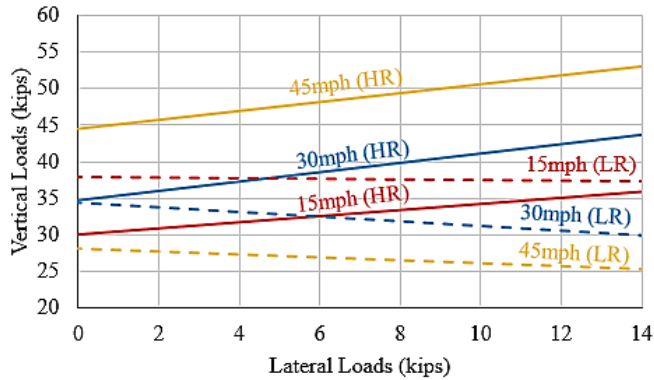


Figure 13. Correlation between lateral and vertical axle loads on curved track.

#### 4.2.2 Lateral Rail Displacements

Lateral rail displacements were measured to understand the lateral resistance of the crosstie-fastening system to lateral loading for a particular design. Both the static and dynamic measurements resulted in similar displacement responses (Figure 14). The stiffness of the rail (amount of lateral load required to displace the rail) was almost the same as recorded from the static TLV tests and from train passes. The only significant difference between the static and dynamic displacements is that the web displacements measured in the low rail showed a higher range of values, attributed to the displacement due to an eccentric vertical load. If a similar eccentricity is not matched by a passing axle, this creates an offset.

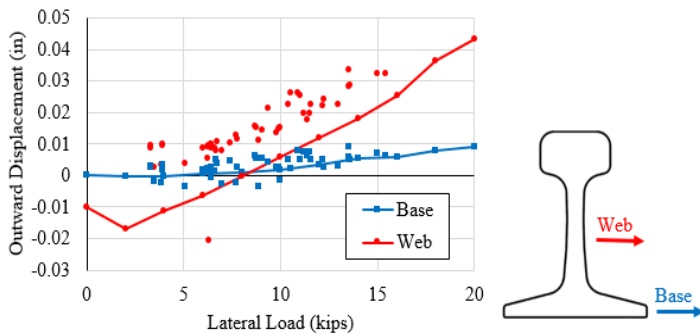


Figure 14: Lateral displacements of the low rail from static and dynamic lateral loads.

Figure 14 also shows the linearity of the lateral loads to rail displacements. This high correlation suggests that the system behaves linearly to input loads, easing the mechanistic and computational analysis of the system. The slopes of these curves

represent compliance (the inverse of the stiffness of the rail to lateral displacement). These compliances were generally uniform and unique to each rail seat. This is a good indicator that there exists a consistent lateral stiffness per rail seat, which can be used in performing parametric analyses (e.g. comparing fastening systems and rail pads).

## 5 CONCLUSIONS

This study provided useful lessons about relationships between vertical and lateral loading under a wide variety of conditions. Vertical loading demands on tangent track showed negligible deviation from nominal wheel loads. Measured impact loads were higher from the lighter-weight passenger consist as a percentage of nominal wheel loads than the freight consist (150% to 125%) and occurred more frequently as a percentage of total axles (6% to 3%). Neglecting the effects of impact loads, the vertical loads did not vary as a function of train speed on tangent track.

Vertical loading demands on curved track were significantly higher than on tangent track. At an overbalanced speed of 45mph, vertical wheel loads on the high rail exceeded the nominal wheel load by 40% from the centrifugal forces acting on the body of the railcar to shift the weight nearer to the high rail. At the same speed, loads on the low rail were reduced by 20% of the nominal wheel load, which represents a higher L/V ratio as lateral forces remained relatively consistent.

Vertical crosstie displacements suggested high variability of stiffness within the curved section, with high rail displacements being 40% lower than low rail displacements for the same input loads. From vertical tie deflections, compressive stresses at the crosstie-ballast interface were approximated to span a wide range of seven to nine crossties. Assuming uniform stiffness across the same ends of adjacent crossties, crosstie-ballast stresses at the center crosstie accounts for 20 to 30% of the load, and the center three crossties account for 50 to 70%. These static deflections also represented the maximum magnitude of deflections when compared with dynamic tie displacements.

Typical rail seat forces measured from a freight consist on tangent track ranged from 44-56% of the vertical wheel load. However, with low substructure stiffness and/or slack below a particular rail seat, transfer forces were generated as low as 15%. In all cases, higher substructure stiffness (low crosstie deflections) resulted in higher rail seat loads. In the

most extreme case of static loads as high as 95% of the wheel load was transferred to the rail seat on the high rail of a curved track. On the low rail 25% of the load was transferred to the rail seat with the same loading conditions and tie deflections measured 40% higher. The variability of rail seat forces also increased with increasing speed, as vertical loads are more susceptible to increases from vehicle dynamics.

Vertical web strains suggest a slightly smaller zone of influence than the crosstie displacements (about five crossties). The vertical compressive stresses in the web above the center crosstie represents about 65% of the total load transferred within the rail web. This represents the undamped flow of forces above the rail base.

Lateral loading demands are significantly higher on curved track than tangent track, with median lateral loads two to five times as high as those on tangent track. In contrast to tangent track, lateral loads show a significant dependence on train speed for curved track. On the high rail, as train speeds exceed balancing speed the lateral loads double with respect to the lower speed magnitudes, which are already twice as high as lateral loads measured on tangent track. On the low rail, lateral loads are 2.5 times as high as those on tangent track and decrease slightly with increasing train speed.

The lateral displacements of the rail base and web were closely correlated to lateral wheel loads. This suggests a lateral stiffness exists unique to the rail seat, which can be used in parametric studies to compare factors that influence resistance to rail translation and rotation. Also, measured web displacements were 4 times larger than base displacements, suggesting significant rigid body rotation of the rail.

#### ACKNOWLEDGEMENTS

Funding for this research effort has been provided by the Federal Railroad Administration (FRA), part of the United States Department of Transportation (US DOT). The published material in this report represents the position of the authors and not necessarily that of DOT. We have also received generous support and guidance from our industry partners: Union Pacific Railroad; BNSF Railway; National Railway Passenger Corporation (Amtrak); Amsted RPS / Amsted Rail, Inc.; GIC Ingeniería y Construcción; Hanson Professional Services, Inc.; and CXT Concrete Ties, Inc., an LB Foster Company. We also thank Harold Harrison; Vince Peterson from CXT

Concrete Ties, Inc.; Tim Crouch from the Monticello Railway Museum; Steve Mattson from VAE Nortrak North America, Inc.; and Ryan Kernes, Thomas Frankie, Jacob Henschen, Tim Prunkard, Darold Marrow, and Marc Killion from the University of Illinois for their work and guidance on this project.

#### REFERENCES

- (1) International Heavy Haul Association (IHHA). Guidelines to Best Practices for Heavy Haul Railway Operations, Infrastructure Construction and Maintenance Issues. D. & F. Scott Publishing, Inc. North Richland Hills, Texas, 2009.
- (2) FIB, 2006, Precast concrete railway track systems. International Federation for Structural Concrete (fib). Sprint-Digital-Druck. Stuttgart, Germany.
- (3) Zeman, J.C., Hydraulic Mechanisms of Concrete Tie Rail Seat Deterioration, M.S., University of Illinois at Urbana-Champaign, Urbana, Illinois, 2010.
- (4) Van Dyk et al 2012, International Concrete Crosstie and Fastening System Survey – Final Results, University of Illinois at Urbana-Champaign, Results Released June 2012
- (5) Hanna, Amir, 1975, Railway Track Research – Theoretical and Experimental. Portland Cement Association 1975. Skokie, IL.
- (6) Van Dyk, B. J., et al., 2009, Considerations for the Mechanistic Design of Concrete Sleepers and Elastic Fastening Systems in North America. Paper presented at the Proceedings of the International Heavy Haul Association Conference, IHHA 2013.
- (7) ARA, Inc., ERES Consultants Division, Guide for Mechanistic-Empirical Design of New and Rehabilitated Pavement Structures, Champaign, Illinois 2004.
- (8) Ahlbeck, D., M. Johnson, H. Harrison, & R. Prause, 1976. Pilot Study for the Characterization and Reduction of Wheel/Rail Loads. U.S. Department of Transportation, Springfield, VA.
- (9) APTA Commuter Rail Executive Committee, 14. APTA SS-M-014-06: Standard for Wheel Load Equalization of Passenger Railroad Rolling Stock, The American Public Transportation Association, Washington, D.C. 2007.
- (10) Prause, R. H., & Kish, A., 1978, Statistical Description of Service Loads for Concrete Cross Tie

Track, 57<sup>th</sup> Annual Meeting of the Transportation Research Board, January 1978.

(11) Moody, Howard G., 1987, Dynamic Wheel Load Detector Extends Life of Railroad Ties. TR News, (January-February 1987), pp. 8-9.

(12) Harrison, H. D., et al., 1984, Correlation of Concrete Tie Track Performance in Revenue Service and at the Facility for Accelerated Service Testing, FRA/ORD-84/02.1, Federal Railroad Administration, Washington, D.C., August 1984

(13) Reiff, R., 2009a, "Evaluation of Concrete Tie Rail Seat Abrasion Detection/Measurement Systems," AAR Research Report RS-09-001.

(14) Anderson, J. S., & Rose, J. G., 2008, In-situ test measurement techniques within railway track structures. Paper presented at the Proceedings of the ASME/IEEE/ASCE Joint Rail Conference, JRC 2008, 187-207.

(15) Hay, W.W., 1982. Railroad Engineering, 2nd ed., John Wiley & Sons, Inc., New York City, New York, Ch. 23, pg. 253 and 448.

(16) Sadeghi, J., 2008, Experimental evaluation of accuracy of current practices in analysis and design of railway track sleepers. Canadian Journal of Civil Engineering, 35 (9), pp. 881-893

(17) AREMA Manual for Railway Engineering, 2009, American Railway Engineering and Maintenance-of-Way Association (AREMA), Landover, Maryland, v 1, Ch. 30.

(18) Handbook of Railway Vehicle Dynamics, 2006, CRC Press, Taylor & Francis Group, Boca Raton, Florida, pp. 212.